Optimizing Molecule-Like Gold Clusters for Light Energy Conversion

Kevin G. Stamplecoskie and Abigail Swint

Notre Dame Radiation Laboratory, University of Notre Dame, Notre Dame, Indiana, 46556, United States

Abstract. *Atomically precise gold clusters that are less than ~1 nm in diameter are emerging as a new class of light absorbing material for harvesting solar energy. Herein, we explore the size dependent properties of glutathione-protected clusters, ($Au_{25}GSH_{18}$, $Au_{18}GSH_{14}$, $Au_{15}GSH_{13}$ and $Au_{11}GSH_{11}$) in sensitizing mesoscopic TiO_2 films. The excited state properties of gold clusters are correlated with the photovoltaic performance of metal cluster sensitized solar cell. $Au_{18}GSH_{14}$ exhibit the highest photoconversion efficiency. The size dependent photovoltaic results are rationalized based on optimizing both the light absorption of the clusters as well as the size dependent excited state behavior.*

Introduction

Metal nanoparticles support plasmon absorptions, which have extremely short excited state lifetimes (~1 ps).[1-2] By contrast, gold and silver clusters that are <1 nm in diameter have long-lived, molecule-like excited states.[3-14] These atomically precise gold and silver clusters have emerged as a new class of light harvesting materials.[15-20] Metal clusters display intense photoluminescence, with excited state lifetimes of hundreds of nanoseconds to microseconds.[5-6, 21-23] The long-lived excited state allows for charge injection into large bandgap semiconductors like TiO_2, used in solar cells and water splitting photocatalysts.[16-19, 24-25] In particular, thiol (SR) protected gold clusters have been recently investigated for solar cells due to these

favorable excited state properties, as well as their apparent photostability under long periods of excitation.[16, 18-19]

The optical properties (absorption spectrum and excited state lifetime) of individual Au_xSR_y clusters are strongly dependent upon; (1) the exact number of gold atoms (ie. Au_{11}, Au_{15}, Au_{18}, Au_{25}), and (2) the choice of thiol used to stabilize the clusters (ie. glutathione, phenylethane thiol, mercaptopropionic acid etc...).[3, 5, 26] The shape and particular stability of some of these clusters has been predicted using 'magic numbers'.[14] However, using magic numbers as a predictor, $Au_{25}GSH_{18}$ is considered to be stable in the -1 oxidation state, whereas those clusters oxidize readily to a stable neutral charged species when exposed to air.[27-28] The shape, structural stability and how this relates to their excited state properties are a newly evolving area of research.

With respect to light harvesting, the ability to absorb a large fraction of the solar spectrum, as well as the ability of the excited state to transfer an excited electron to the metal oxide support (TiO_2), are both important factors in the overall efficiency. We have previously reported on the excited state properties of a series of different sizes of glutathione protected gold clusters.[3] Other researchers have shown that the ligands can have an equally important role in dictating the excited state properties, (i.e., emission quantum yield and lifetime).[26, 29] Electron donating ligands like glutathione have been shown to give a high quantum yield of emission and long-lived excited state, both of which are useful in maximizing electron transfer from the excited state, and therefore, maximizing light harvesting efficiency.[26, 29]

Herein we investigate solar cell efficiencies of a series of glutathione (GSH) protected gold clusters; $Au_{11}GSH_{11}$, $Au_{15}GSH_{13}$, $Au_{18}GSH_{14}$ and $Au_{25}GSH_{18}$. Each of these clusters has different absorption spectra, but also different dynamics of their excited states. Previous reports on several of these clusters have delivered lower efficiency of light harvesting, making it difficult to draw conclusions about the relative ability of each cluster in light harvesting.[25, 30] Herein, the photovoltaic performance of each cluster is discussed with respect to their ability to absorb a

broad spectrum of sunlight as well as their relative ability to convert absorbed photons into photocurrent, which is governed by excited state lifetime and electron transfer properties.

Results and Discussion

The synthesis of Au_xGSH_y clusters and solar cell fabrication is discussed in detail in the experimental section. Absorption spectra for each of the different clusters in aqueous solution (Figure 1) correspond to the reported spectra for these clusters.[3, 31] Mass spectroscopy was also used to characterize the clusters and confirm the identity of each (Figure S1).[3, 31]

To sensitize solar cells with various clusters, TiO_2 electrodes were immersed in aqueous solutions containing Au_xGSH_y clusters at pH = 4, to maximize loading onto TiO_2. For comparison of loading, electrodes with only transparent active layers of TiO_2, (no scattering layer, Figure 1B inset) were prepared and immersed in the same cluster solutions. Absorption spectra of active layers sensitized with $Au_{11}GSH_{11}$, $Au_{15}GSH_{13}$, $Au_{18}GSH_{14}$ and $Au_{25}GSH_{18}$ are shown in Figure 1B, along with an image of the corresponding active layers. The relative absorption spectra for
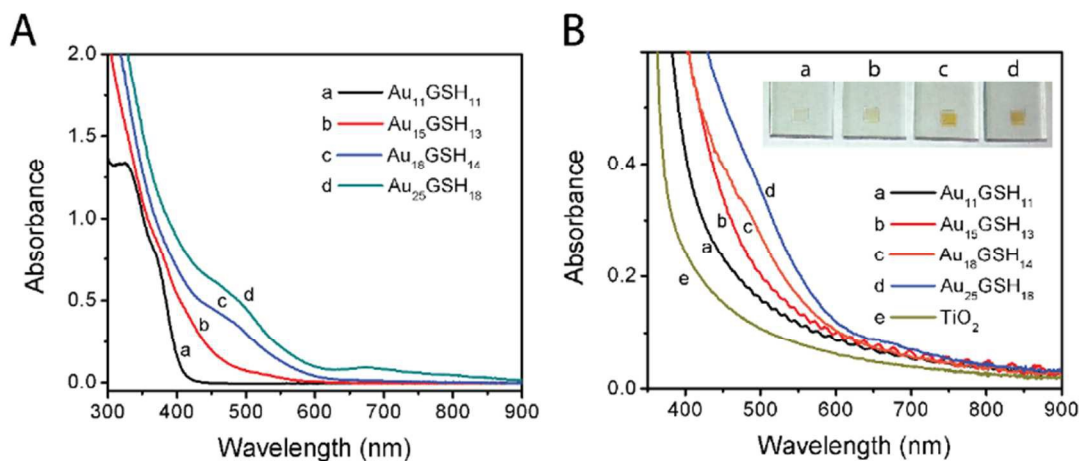

Figure 1. A) Absorbance spectra of aqueous solutions of clusters and B) absorbance spectra of glutathione protected clusters adsorbed onto TiO_2 films, (used as active layers for solar cells). The inset is an image of solar cells with each of the different sizes of glutathione-protected clusters as sensitizers.

each of the sensitizers in solutions matches well with the relative absorption spectra of active layers, indicating similar surface coverage by each of the sensitizers.

From the absorption properties alone, it is expected that the $Au_{25}GSH_{18}$ clusters absorb the most light and, therefore, should provide the highest photocurrents and solar cell efficiencies. This is in fact not the case. Figure 2 shows the results of photovoltaic performance for MCSSC sensitized with each of the clusters, and for TiO_2 alone (no sensitizer) for comparison. The photovoltaic parameters; efficiency (η), short circuit current (I_{sc}), open circuit voltage (V_{oc}), fill factor (FF) and maximum power (P_{max}) are summarized in Table 1.

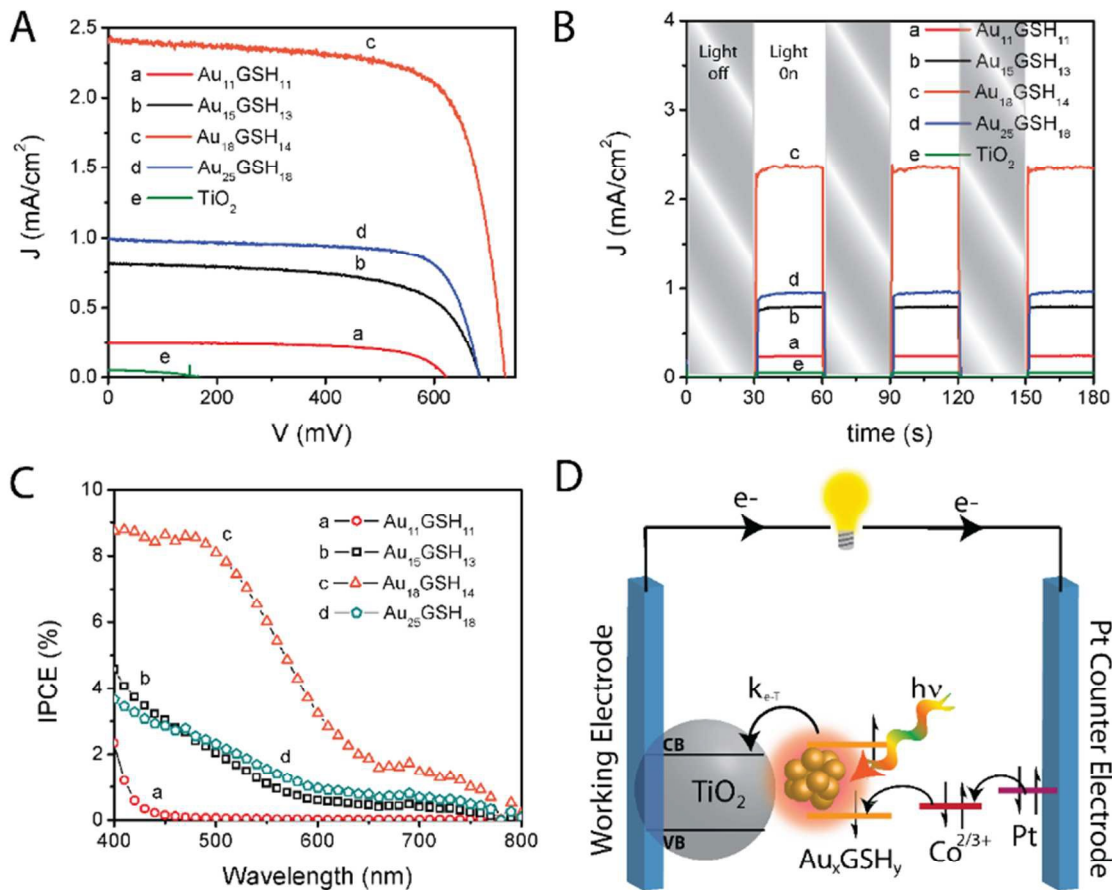Figure 2. Representative photocurrent versus applied voltage A) and photocurrent versus time with light on/off cycles as indicated B), illustrating the efficiency and stability of the cluster sensitized solar cells. C) Incident photon to current efficiency measured for each of the MCSSC. D) Illustration of the electron transfer to TiO_2 (k_{e-T}) and several other important electron transfer processes in MCSSC.

5

The maximum efficiency obtained from these photoelectrochemical mesurements was 1.61 % obtained with the $Au_{18}GSH_{14}$ as the sensitizer. An average of 6 solar cells were constructed and tested for each sensitizer, and the efficiency of $Au_{18}GSH_{14}$ was consistently higher. Others have reported maximum light harvesting efficiencies of only 0.26 % for atomically precise, glutathione protected gold clusters.[25, 30] $Au_{25}GSH_{18}$ clusters have light absorption that extends into the NIR, and it was previously thought that this extended light absorption was the critical property of these clusters in maximizing light harvesting efficiency. From the IPCE results in Figure 2C, we see that the photocurrent response for $Au_{18}GSH_{15}$ with significant absorption in the visible offers the best features for maximizing light harvesting as well as light conversion efficiency.

Table 1. Summary of photovoltaic parameters for solar cells sensitized with glutathione-protected clusters

Au_xGSH_y	η_{max} (%)	$\eta_{average}$ (%)	V_{OC} (mV)	I_{SC} (mA/cm^2)	FF	P_{max} (μW)
$Au_{25}GSH_{18}$	1.02	0.88 ± 0.21	623 ± 8	2.54 ± 0.48	0.55 ± 0.04	100 ± 6
$Au_{18}GSH_{14}$	**1.61**	**1.50 ± 0.10**	**710 ± 7**	**3.20 ± 0.67**	**0.60 ± 0.04**	**161 ± 11**
$Au_{15}GSH_{13}$	0.49	0.37 ± 0.08	657 ± 12	0.91 ± 0.10	0.62 ± 0.06	41 ± 10
$Au_{11}GSH_{11}$	0.30	0.26 ± 0.06	649 ± 19	0.59 ± 0.09	0.65 ± 0.10	28 ± 6
TiO_2 blank	0.03	0.02 ± 0.01	290 ± 150	0.14 ± 0.11	0.02 ± 0.01	2.2 ± 1.7

*Average results for 6 solar cells for each gold cluster sensitizer.

The maximum photocurrent (I_{SC} and IPCE), and open circuit voltage (V_{OC}), correlate with overall efficiency, where $Au_{18}GSH_{14}$ clusters outperform the other sensitizers. In general, photocurrent scales with light absorption.[32-33] Herein this is true as well, except for the case of $Au_{25}GSH_{18}$, which has the most light absorption (Figure 1), but not the highest photocurrent or overall efficiency. What then is limiting the attainable photocurrent for $Au_{25}GSH_{18}$ clusters?

We have previously reported the excited state lifetimes of the clusters that are used in this study.[3] Time-resolved femtosecond transient absorption measurements provide insights into the nature of the excited state and its

deactivation processes. The technique allows us to monitor the excited state and how it relaxes between ~100 fs – 2000 ps after excitation.[3, 6, 21, 34-35] The excited state absorption spectrum 1 ps after 387 nm laser pulse excitation, and excited state time decay monitored at 500 nm are shown in Figure 3.
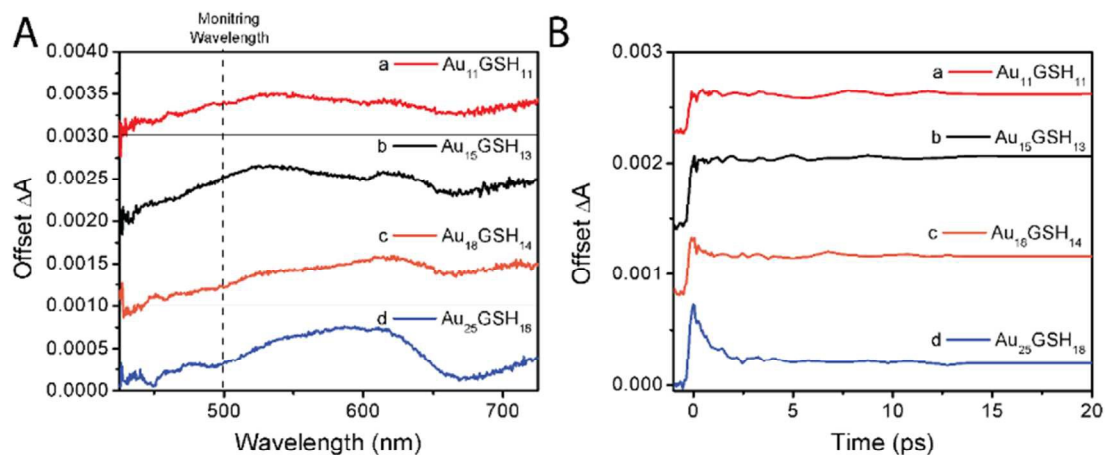

Figure 3. A) Excited state absorption spectrum (ΔA) of $Au_{11}GSH_{11}$, $Au_{15}GSH_{13}$, $Au_{18}GSH_{14}$, and $Au_{25}GSH_{18}$, recorded 1 ps after 387 nm, 130 fs FWHM laser pulsed excitation, and B) excited state relaxation as a function of time, recorded at 500 nm (Adapted from reference 3).

The induced absorption shown Figure 3A is a characteristic of the excited state of gold clusters, similar for all of the clusters. The absorption of the excited state monitored at 500 nm shows no decay at all for the smallest clusters and an increasing rapid relaxation component with increasing cluster size (Figure 3B).

The efficiency of TiO_2 sensitized solar cells is governed by the kinetics of many electron transfer processes.[35-36] For example, electron injection from the excited state of sensitizers into TiO_2 competes kinetically with the normal relaxation processes in the sensitizer. The competitive kinetic processes are illustrated in Scheme 1, where k_{e-T} represents the rate constant for electron transfer from excited clusters into TiO_2 and k_1 and k_2 represent excited state relaxation processes in the glutathione protected clusters. For small clusters ($Au_{11}GSH_{11}$ and $Au_{15}GSH_{13}$) there is no short lifetime component (k_1) depleting their excited state population, for $Au_{18}GSH_{14}$ there is only a small fraction (30 %) of the excited state that decays

rapidly, and for $Au_{25}GSH_{18}$ ~70 % of the excited state decays within the first 3 ps after excitation (Figure 3B).

Scheme 1. Illustration of the relaxation of the excited state of gold clusters (k₁ and k₁) and competing electron transfer to TiO₂ (k_{et})
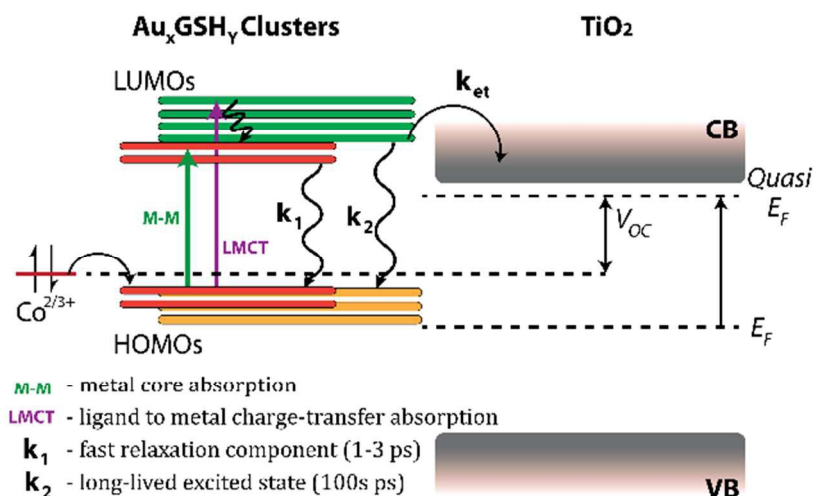
In order to determine the rate of electron transfer (k_{e-T}) from clusters into TiO_2, we employed femtosecond transient absorption. Clusters were adsorbed directly onto TiO_2 active layers as shown in the inset in Figure 1B, and placed in an inert atmosphere (vacuum sealed cuvettes). The decay of the excited state after femtosecond laser pulse excitation was then monitored at 550 nm. As a blank, clusters were adsorbed onto glass, which is an insulating material where electron transfer cannot occur. A comparison of the excited state relaxation on glass and on TiO_2 is shown in Figure S2 in the supporting information. Fitting the data with the normal relaxation without electron transfer (Amplitude: A_1 and lifetime: τ_1) as well asl an extra relaxation component corresponding to electron transfer (Amlitude: A_2 and lifetime: τ_2) yields the lifetimes listed in Table 2, as well as the rate constants for electron transfer (reciprocal of τ_2). The rate constants for electron transfer are not statistically different, with values of 1-2 $\times 10^{10}$ s^{-1}. Therefore, it is not the rate of electron transfer that is limiting the efficiency of $Au_{25}GSH_{18}$.

Table 2: Fitting Parameters for the Relaxation of Au$_x$GSH$_y$ Adsorbed on TiO$_2$ and Corresponding Electron Transfer Rate Constants (k$_{e-T}$)*

Cluster	A$_1$	τ$_1$ (ps)	A$_2$	τ$_2$ (ps)	*k$_{e-T}$ x10^{10} (s^{-1})
Au$_{25}$GSH$_{18}$	0.31	2.14	0.42	53.5 ±8.3	1.9 ±0.3
Au$_{18}$GSH$_{15}$	0.13	0.7	0.19	72.8 ±14.6	1.4 ±0.3
Au$_{15}$GSH$_{13}$	N/A	N/A	0.08	76.5 ±53.6	1.3 ±0.9
Au$_{11}$GSH$_{11}$	N/A	N/A	0.18	78.4 ±45.1	1.3 ±0.7

*k$_{e-T}$ was calculated as the inverse of the time constant (τ$_2$) associated with electron transfer to TiO$_2$ (see Supporting Information).

Clusters have two relaxation components for their excited state, one component measured by femtosecond transient absorption to be on the order of 1-3 ps (Table 2) and a longer charge transfer component that is several hundred nanoseconds.[3, 6] Electron injection, that happens on the order of 100 ps, cannot compete with this 1-3 ps relaxation process, and so most of the excited state of Au$_{25}$GSH$_{18}$ relaxes without contributing to photocurrent in a working solar cell. Our previous study showed that the photocatalytic activity for electron transfer to methyl viologen, under equivalent excitation, is similar for Au$_{18}$GSH$_{14}$ and Au$_{15}$GSH$_{13}$. However, sunlight does not provide equivalent excitation to these two compounds. The experiments performed here measure solar cells excited with AM 1.5 (100 mW/cm^2) with a spectrum matching solar radiation. Figure 4A shows an absorption spectrum of Au$_{25}$GSH$_{18}$ and the AM 1.5 solar flux (photons/s/m^2). The overlapping area under these two curves is what contributes to photocurrent in a solar cell. A method of predicting maximum attainable photocurrents (ie. J$_{max}$ for 100 % IPCE) is to simply multiply the solar flux (S.F.) at each wavelength by the absorbance of the material at that wavelength (Abs), converting that to current in mA/cm^2 and integrate over the entire solar spectrum, Equation (1).

$$J_{max} = \int Absorbance_\lambda \cdot Solar\ Flux\ (photons/cm^2/s)/\ 6.314\ x10^{18}\ (e^-/A) \qquad (1)$$
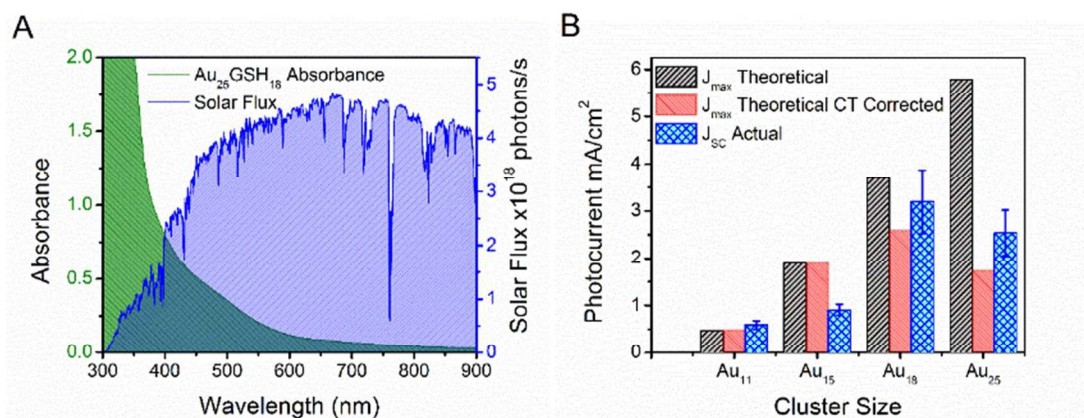

Figure 4. A) Absorption spectrum of $Au_{25}GSH_{18}$, and solar flux for AM 1.5, and B) maximum theoretical photocurrent for each size of clusters considering only overlap of light absorption with solar flux (J_{SC} Theoretical) and with only the charge transfer excited state lifetime capable of contributing (J_{SC} Theoretical CT Corrected), overlaid with actual short circuit current measurements for each MCSSC (J_{SC} Actual).

This analysis assumes that every photon absorbed leads to photocurrent. There are many processes involved in a solar cell that can reduce this maximum photocurrent, including back electron transfer from TiO_2 to clusters, or electron transfer from TiO_2 to the oxidized form of the redox couple in the electrolyte. For simplicity, we assume that these contributions are minimal and calculate J_{max} Theoretical, shown in Figure 4B.

To correct for the rapid relaxation component in Au_{25} and Au_{18} clusters, that does not contribute to short circuit current (electrons that relax before injecting into TiO_2), J_{max} Theoretical is multiplied by the proportion of the excited state that corresponds to the long-lived charge-transfer state (ie. 0.3 for $Au_{25}GSH_{18}$, 0.7 for $Au_{18}GSH_{15}$, and 1.0 for both $Au_{15}GSH_{13}$ and $Au_{11}GSH_{11}$) to give 'J_{max} Theoretical CT Corrected'. There is a strong correlation between J_{max} Theoretical CT Corrected and the J_{SC} Actual (measured photocurrent in solar cells), as shown in Figure 4B. In other words, when only light absorption is considered, the model predicts increasing photocurrent with increasing light absorption as expected, but does not match well with the trend seen in light harvesting. However, when the excited state behavior of

the clusters is considered, where only the long-lived components of the excited state can contribute to photocurrent, there is a good correlation between expected and actual photocurrents. Furthermore, the calculation takes into account the absorbed photons for each active layer, and predicts maximum efficiency. A good correlation between excited state lifetime and photocurrent indicates that it is electron transfer to TiO_2 that is limiting the efficiency of these solar cells, and not other processes like electron transfer with the redox electrolyte. It is important to note that the cobalt electrolyte provides improved light harvesting efficiencies in this study, and that it limited coverage of TiO_2 and not electron transfer, is a major barrier to reaching even higher overall light harvesting.

Au$_{18}$GSH$_{14}$ provides the highest solar cell efficiencies because it combines good light absorption across the visible spectrum, with a long excited state lifetime capable of injecting electrons into TiO_2. When a sensitizer injects electrons into TiO_2 the quasi-Fermi level of the electrode is increased. Sensitizers with a stronger ability to inject electrons into TiO_2 form a more charge-separated state, provide higher quasi-Fermi level and an increased V$_{OC}$ (illustrated in Scheme 1).[37] For this reason, solar cells sensitized with Au$_{18}$GSH$_{14}$ have a higher average V$_{OC}$ (710 mV) than for the other MCSSC (Table 1).

In summary, a series of different sizes of glutathione protected gold clusters were employed as light absorbing materials to sensitize liquid junction, TiO_2 solar cells. It was found that Au$_{18}$GSH$_{14}$ provide the highest conversion efficiency for sunlight, achieving a maximum efficiency of 1.6 %. These clusters combine good light absorption and a long-lived excited state capable of efficient electron injection into TiO_2. Gold clusters are emerging as a new light harvesting material for various applications in photocatalysis.[15, 24] For photocatalysis and light harvesting, strong absorption of solar radiation is favorable. This work highlights the fact that good light absorption is not the only factor to consider in the search for efficient light harvesting materials. For the gold clusters used herein, a slow rate of relaxation of the excited state is critical to achieve efficient electron injection and high photocurrents in these MCSSC. A predictive model is used to understand the

11

efficiency of solar cells that combines light absorption and excited state behavior. This model is important, not only for cluster sensitized solar cells, but as a general model for all metal oxide sensitized solar cells.

Experimental

Cluster Synthesis

Glutathione protected particles were synthesized using a previously reported method.[31] Briefly, 0.2 g of gold (III) chloride trihydrate (99.9%, Sigma-Aldrich) and 0.31 g of L - glutathione (reduced, 98%, Sigma-Aldrich) were mixed in 100 mL deionized water (DI water) at room temperature and was kept stirring until a colorless solution was obtained. 20 mL of the solution was used for each of the samples of different sizes of clusters and the pH was changed to 7, 9, 10, and 11 with sodium hydroxide (0.995, Sigma-Aldrich), for $Au_{11}GSH_{11}$, $Au_{15}GSH_{13}$, $Au_{18}GSH_{14}$ and $Au_{25}GSH_{18}$, respectively. Each solution was then purged with carbon monoxide for 2 minutes and was allowed to reduce overnight. Clusters were characterized by UV-vis absorption and mass spectrometry after at least 24 hours.[3]

Cluster Purification

Each of the Au_xGSH_y solutions were purified of excess glutathione and sodium ions using centrifugal filter units (Amicon Ultra – 15 Centrifugal Filters, Ultracel – 3K). When centrifuged at 3500 RCF, the units allowed the excess glutathione and sodium ions through the filter while keeping a concentrated solution of Au_xGSH_y clusters. 15 mL of each solution was added to separate filter units and centrifuged/washed with milli-Q water, and 5 mL of clean, concentrated solution were obtained. Purifying and concentrating the solutions provided higher loading and better sensitization of the TiO_2 electrodes.

Solar Cell Fabrication

Solar cells were fabricated using a method previously reported.[19] The fluorine doped tin oxide coated glass (FTO), (Pilkington TEC Glass-TEC 8, Solar 2.3 mm thickness) used for the counter and working electrodes, were cleaned in a

detergent solution with ultrasonic bath, rinsed with deionized water and ethanol, and held at 500°C to remove any organics. Counter electrodes were prepared by coating with two drops of H_2PtCl_6 solution (2 mg in 1 mL of ethanol) on cleaned FTO and sintered at 400 °C for 15 min to form a Pt^0 counter electrode. For the working electrodes, the FTO was immersed in 40 mM $TiCl_4$ (aqueous) at 70 °C for 30 min and rinsed with water and acetonitrile. A transparent nanocrystalline active layer of TiO_2 (0.125 cm^2) was then prepared on the FTO glass by a doctor blade technique using TiO_2 paste (Solaronix, Ti-Nanoxide T/SP) and dried at room temperature for 1 h, then gradually heated to 80°C for 1 h followed by 500°C for 1 h. A scattering layer containing 400 nm sized anatase TiO_2 particles (CCIC, PST-400C) was deposited over the active layer (0.25 cm^2) by doctor blading as well. The electrode containing the TiO_2 scattering layer was again dried for 1 h at room temperature and heated for 1 h at 80°C then 1 h at 500°C. The TiO_2 electrodes were treated again with 40 mM $TiCl_4$ at 70°C for 30 min and sintered at 500 °C for 30 min.

The TiO_2 electrodes were sensitized with Au_xGSH_y after the second $TiCl_4$ treatment. First, the pH of each Au_xGSH_y solution was changed to 4 using a 10:1 mixture of deionized water and acetic acid. Immediately after, the electrodes were submerged in the solution for 5 minutes. Once removed, the electrodes were rinsed with deionized water and ethanol and allowed to dry at room temperature.

The Au_xGSH_y sensitized TiO_2 electrode and Pt-counter electrode were assembled into a cell by heating at 200 °C with a hot-melt ionomer film (Surlyn SX 1170-25, Solaronix) as a spacer between the electrodes. A drop of electrolyte solution (acetonitrile containing 0.22 M $Co(bpy)_3(PF_6)_2$, 0.033 M $Co(bpy)_3(PF_6)_3$, 0.1 M $LiClO_4$, and 0.5 M 4-tertbutylpyridine) was placed over a hole drilled in the counter electrode of the assembled cell and driven into the cell via vacuum backfilling. The hole was then sealed using additional Surlyn and a cover glass (0.1 mm thickness). Finally, indium metal soldered to contact points of the working and counter electrodes.

Solar Cell Photoelectrochemical Performance

Samples were irradiated with AM 1.5 (100 mW/cm^2) solar radiation by using a Xe lamp, an AM 1.5 filter, and placing cells at an appropriate distance where 100 mW/cm^2 illumination power was obtained. A Princeton Applied Research model PARSTAT 2263 was used for recording J vs V, I vs time and V vs time curves. A Newport Oriel QE Kit (QE-PV-SI) was used for measuring IPCE spectra.

*Femtosecond Pump-Probe Spectroscopy for Characterizing Au$_x$GSH$_y$ Excited States*

Ultrafast transient absorption techniques were performed using a Clark laser with a 775 nm fundamental pulsed at 1 kHz with 130 fs FWHM pulse durations. The fundamental is split to generate a white light probe by focusing through a CaF$_2$ crystal generating 380-800 nm light. For 387 nm excitation the second harmonic of the 775 nm is generated and used to excite samples. In this pump-probe setup, the transient absorption spectrum is recorded as a difference between probe signals with/without a pump pulse, and the delay between pump and probe is controlled to generate spectra at varied times following excitation.

Acknowledgements

Supporting Information. Mass spectrometer identification of clusters sizes, and transient absorption decay traces for each size of clusters with quenching of excited state lifetimes with TiO$_2$ are available.

14

TOC Graphic & Statement
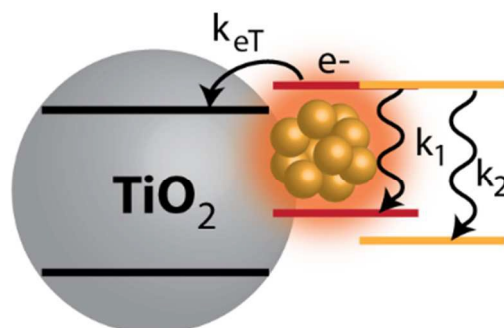
As light harvesting materials, $Au_{18}SR_{14}$ metal clusters are highlighted for their favourable excited-state properties leading to better photovoltaic performance.

References

1.   Hartland, G. V., Optical Studies of Dynamics in Noble Metal Nanostructures. *Chem. Rev.* **2011,** *111*, 3858-3887.

2.   Stamplecoskie, K. G.; Manser, J. S., Facile SILAR Approach to Air-Stable Naked Silver and Gold Nanoparticles Supported by Alumina. *ACS Applied Materials & Interfaces* **2014,** *6*, 17489-17495.

3.   Stamplecoskie, K. G.; Kamat, P. V., Size-Dependent Excited State Behavior of Glutathione-Capped Gold Clusters and Their Light-Harvesting Capacity. *Journal of the American Chemical Society* **2014,** *136*, 11093-11099.

4.   Aikens, C. M.; Li, S. Z.; Schatz, G. C., From Discrete Electronnic States to Plasmons: TDDFT Optical Absorption Properties of $Ag_{(n)}$ n = 10, 20, 35, 56, 84, 120) Tetrahedral Clusters. *J. Phys. Chem. C* **2008,** *112*, 11272-11279.

5.   Devadas, M. S.; Kim, J.; Sinn, E.; Lee, D.; Goodson, T.; Ramakrishna, G., Unique Ultrafast Visible Luminescence in Monolayer-Protected Au_{25} Clusters. *J. Phys. Chem. C* **2010,** *114*, 22417-22423.

6.   Stamplecoskie, K. G.; Chen, Y. S.; Kamat, P. V., Excited-State Behavior of Luminescent Glutathione-Protected Gold Clusters. *J. Phys. Chem. C* **2014,** *118*, 1370-1376.

7.   Tlahuice, A.; Garzón, I., On the structure of the $Au_{18}(SR)_{14}$ cluster. *Phys. Chem. Chem. Phys.* **2012,** *14*, 3737.

8.   Negishi, Y.; Nobusada, K.; Tsukuda, T., Glutathione-Protected Gold Clusters Revisited: Bridging the Gap Between Gold(I)-Thiolate Complexes and Thiolate-Protected Gold Nanocrystals. *J. Am. Chem. Soc.* **2005,** *127*, 5261-5270.

9.   Philip, R.; Chantharasupawong, P.; Qian, H.; Jin, R.; Thomas, J., Evolution of Nonlinear Optical Properties: From Gold Atomic Clusters to Plasmonic Nanocrystals. *Nano Lett.* **2012,** *12*, 4661-4667.

10.   Stamplecoskie, K. S.; Scaiano, J. C., Kinetics of the Formation of Silver Dimers: Early Stages in the Formation of Silver Nanoparticles *J. Am. Chem. Soc.* **2011,** *133*, 3913-3920.

11.   Negishi, Y.; Nakazaki, T.; Malola, S.; Takano, S.; Niihori, Y.; Kurashige, W.; Yamazoe, S.; Tsukuda, T.; Häkkinen, H., A Critical Size for Emergence of Nonbulk Electronic and Geometric Structures in Dodecanethiolate-Protected Au Clusters. *Journal of the American Chemical Society* **2014,** *137*, 1206-1212.

12.   Zhu, M.; Aikens, C. M.; Hollander, F. J.; Schatz, G. C.; Jin, R., Correlating the crystal structure of a thiol-protected Au_{25} cluster and optical properties. *J. Am. Chem. Soc.* **2008,** *130*, 5883-5.

13.   Link, S.; El-Sayed, M.; Schaaff, T.; Whetten, R., Transition from nanoparticle to molecular behaviour: a femtosecond transient absorption study of a size selected 28 atom gold cluster. *Chem. Phys. Lett.* **2002,** *356*, 240-246.

14.   Aikens, C. M., Electronic Structure of Ligand-Passivated Gold and Silver Nanoclusters. *J. Phys. Chem. Lett.* **2011,** *2*, 99-104.

15.   Kamat, P. V., Emergence of New Materials for Light–Energy Conversion: Perovskites, Metal Clusters, and 2-D Hybrids. *The Journal of Physical Chemistry Letters* **2014,** *5*, 4167-4168.

16.   Changlin, Y.; Li, G.; Kumar, S.; Kawasaki, H.; Jin, R., Stable $Au_{25}(SR)_{18}/TiO_2$ Composite Nanostructure with Enhanced Visible Light Photocatalytic Activity. *J. Phys. Chem. Lett.* **2013,** *4*, 2847-2852.

17.   Chen, W.; Hsu, Y.; Kamat, P. V., Realizing Visible Photoactivity of Metal Nanoparticles: Excited-State Behavior and Electron-Transfer Properties of Silver (Ag_8) Clusters. *J. Phys. Chem. Lett.* **2012,** *3*, 2493-2499.

18.   Chen, Y. S.; Kamat, P., Glutathione Capped Gold Nanoclusters as Photosensitizers. Visible Light Induced Hydrogen Generation in Neutral Water. *J. Am. Chem. Soc.* **2014,** *136*, 6075-6082.

19.   Chen, Y. S.; Choi, H.; Kamat, P. V., Metal-Cluster-Sensitized Solar Cells. A New Class of Thiolated Gold Sensitizers Delivering Efficiency Greater than 2%. *J. Am. Chem. Soc.* **2013,** *135*, 8822-5.

20.   Devadas, M.; Kwak, K.; Park, J.; Choi, J.; Jun, C.; Sinn, E.; Ramakrishna, G.; Lee, D., Directional Electron Transfer in Chromophore-Labeled Quantum-Sized Au 25Clusters: Au 25as an Electron Donor. *J. Phys. Chem. Lett.* **2010,** *1*, 1497-1503.

21.   Yau, S. H.; Varnavski, O.; Goodson, T., An Ultrafast Look at Au Nanoclusters. *Acc. Chem. Res.* **2013,** *46*, 1506-1516.

22.   Yu, Y.; Luo, Z.; Chevrier, D. M.; Leong, D. T.; Zhang, P.; Jiang, D.; Xie, J., Identification of a Highly Luminescent $Au_{22}(SG)_{18}$ Nanocluster. *J. Am. Chem. Soc.* **2014,** *136*, 1246-9.

23.   Diez, I.; Ras, R. H. A., Fluorescent silver nanoclusters. *Nanoscale* **2011,** *3*, 1963-1970.

24.   Kurashige, W.; Niihori, Y.; Sharma, S.; Negishi, Y., Recent Progress in the Functionalization Methods of Thiolate-Protected Gold Clusters. *The Journal of Physical Chemistry Letters* **2014,** *5*, 4134-4142.

25.   Sakai, N.; Tatsuma, T., Photovoltaic Properties of Glutathione-Protected Gold Clusters Adsorbed on TiO_2 Electrodes. *Advanced Materials* **2010,** *22*, 3185-3188.

26.   Tlahuice-Flores, A.; Whetten, R. L.; Jose-Yacaman, M., Ligand Effects on the Structure and the Electronic Optical Properties of Anionic $Au_{25}(SR)_{18}$ Clusters. *J. Phys. Chem. C* **2013,** *117*, 20867-20875.

27.   Kauffman, D. R.; Alfonso, D.; Matranga, C.; Li, G.; Jin, R., Photomediated Oxidation of Atomically Precise $Au_{25}(SC_2H_4Ph)_{18}^-$ Nanoclusters. *J. Phys. Chem. Lett.* **2012,** *4*, 195-202.

28.   Qian, H.; Sfeir, M. Y.; Jin, R., Ultrafast Relaxation Dynamics of $[Au_{25}(SR)_{18}]^q$ Nanoclusters: Effects of Charge State. *J. Phys. Chem. C* **2010,** *114*, 19935-19940.

29.   Wu, Z.; Jin, R., On the Ligand's Role in the Fluorescence of Gold Nanoclusters. *Nano Lett.* **2010,** *10*, 2568-2573.

30.   Kogo, A.; Sakai, N.; Tatsuma, T., Photoelectrochemical analysis of size-dependent electronic structures of gold clusters supported on TiO_2. *Nanoscale* **2012,** *4*, 4217-4221.

31.   Yu, Y.; Chen, X.; Yao, Q.; Yu, Y.; Yan, N.; Xie, J., Scalable and Precise Synthesis of Thiolated Au_{10-12}, Au_{15}, Au_{18}, and Au_{25} Nanoclusters via pH Controlled CO Reduction. *Chem. Mater.* **2013,** *25*, 946-952.

32.   Santra, P. K.; Kamat, P. V., Tandem-Layered Quantum Dot Solar Cells: Tuning the Photovoltaic Response with Luminescent Ternary Cadmium Chalcogenides. *Journal of the American Chemical Society* **2012,** *135*, 877-885.

33.   Wood, C. J.; Summers, G. H.; Gibson, E. A., Increased photocurrent in a tandem dye-sensitized solar cell by modifications in push-pull dye-design. *Chemical Communications* **2015**.

34.   Cherepy, N. J.; Smestad, G. P.; Grätzel, M.; Zhang, J. Z., Ultrafast Electron Injection: Implications for a Photoelectrochemical Cell Utilizing an Anthocyanin Dye-Sensitized TiO2 Nanocrystalline Electrode. *The Journal of Physical Chemistry B* **1997,** *101*, 9342-9351.

35.   Haque, S. A.; Palomares, E.; Cho, B. M.; Green, A. N. M.; Hirata, N.; Klug, D. R.; Durrant, J. R., Charge Separation versus Recombination in Dye-Sensitized Nanocrystalline Solar Cells: the Minimization of Kinetic Redundancy. *Journal of the American Chemical Society* **2005,** *127*, 3456-3462.

36.   Kamat, P. V., Boosting the Efficiency of Quantum Dot Sensitized Solar Cells through Modulation of Interfacial Charge Transfer. *Accounts of Chemical Research* **2012,** *45*, 1906-1915.

37.   Raga, S. R.; Barea, E. M.; Fabregat-Santiago, F., Analysis of the Origin of Open Circuit Voltage in Dye Solar Cells. *The Journal of Physical Chemistry Letters* **2012,** *3*, 1629-1634.